Evaluation of MVDC Electrical Interties Connecting Remote Communities: an Alaska Case Study

Michele Chamberlin[1], Nathan Green[1], Joules Evergreen[1], Robert Bensin[1],
Stanley Atcitty[2], William Thomson[3], Ingemar Mathiasson[4], and Mariko Shirazi[1]

[1]Alaska Center for Energy and Power, University of Alaska, Fairbanks, AK 99775
[2]Sandia National Laboratories, 1515 Eubank SE, Albuquerque, NM 87123
[3]Alaska Village Electric Cooperative, 4831 Eagle St., Anchorage, AK 99503
[4]Northwest Arctic Borough, 163 Lagoon St., Kotzebue, AK 99752

Technical Report
UAF/ACEP/TP-01-0002
August 2023

Suggested Citation:
M. Chamberlin et al., "Evaluation of MVDC Electrical Interties Connecting Remote Communities: an Alaska Case Study," Alaska Center for Energy and Power, University of Alaska, Fairbanks, 2023. UAF/ACEP/TP-01-0002.
DOI: 10.5281/zenodo.8274640

Notice

This report is available at no cost from the Alaska Center for Energy and Power (ACEP) at the University of Alaska, Fairbanks (UAF) at www.uaf.edu/acep/our-resources/index.php.

This template is based off of the National Renewable Energy Laboratory Report Template, which is available at no cost at www.nrel.gov/comm-standards/editorial/report-template.html.

Cover Photo of solar panels in Shungnak by Michelle Wilber.

Acknowledgments

This research was funded by the Department of Energy (DOE) Office of Electricity (OE) Energy Storage Program, through Sandia National Laboratories. Sandia National Laboratories is a multimission laboratory managed and operated by National Technology & Engineering Solutions of Sandia LLC, a wholly owned subsidiary of Honeywell International Inc. for the U.S. Department of Energy's National Nuclear Security Administration under contract DE-NA0003525. The authors gratefully acknowledge Dr. Imre Gyuk, program manager for the DOE OE Energy Storage Program, for his support of this work.

The authors would like to thank Tom Keister from Resilient Power Systems, Dave Wisniewski from The Okonite Company, and Jody Simoneaux from Wetland Equipment Company for generously providing real-world quotes to enhance the credibility of this work; and Dan Bishop from Golden Valley Electric Cooperative and Clay Koplin from Cordova Electric Cooperative for providing invaluable Alaska utility perspective and enthusiasm. Anonymous reviewers from *Energies* provided edits that shaped the final report. Emilia Sakai Hernandez typeset the final report.

Acronyms

ACEP Alaska Center for Energy and Power

AC Alternating Current

DC Direct Current

HOMER Hybrid Optimization of Multiple Energy Resources

MVDC Medium-Voltage Direct Current

MVAC Medium-Voltage Alternating Current

O&M Operation and Maintenance

PSCAD Power Systems Computer Aided Design

EMTDC Electromagnetic Transients Including Direct Current

LCOE Levelized Cost of Electricity

NAB Northwest Arctic Borough

USD United States Dollar

kWh kilowatt hour

ASHP Air-Source Heat Pumps

PV Photovoltaic

BESS Battery Energy Storage System

AVEC Alaska Village Electric Cooperative

COP Coeffient of Performance

GMD Geometric Mean Distance

GMR Geometric Mean Radius

ACSR Aluminium Conductor Steel-Reinforced cable

AWG American Wire Gauge

NREL National Renewable Energy Laboratory

kV kilovolt

Abstract

Islanded power systems are generally exposed to higher expenses and more grid stability challenges compared to larger interconnected power grids. The interconnection of islanded power systems can lead to numerous advantages. In this work, the techno-economic modeling of the interconnection of two remote communities is presented to explore the feasibility and the economic advantages of an electrical intertie, as well as the challenges from a technical perspective. The unique case study explores two different intertie voltage levels for an AC and a DC intertie. Installation cost estimates were obtained for each intertie case as well as the necessary upgrade costs to keep the system unconnected. These scenarios were simulated using HOMER Pro energy balance models of the system with and without energy storage. The study considers the voltage drop and the power loss along the 25-mile intertie for the power balance modeling process. It is found that with available cost estimates the MVDC intertie economically outperforms the MVAC intertie as well as the current standalone configuration of the modeled islanded power systems. **The MVDC intertie scenario outperforms the standalone configuration even with the inclusion of the energy storage required to increase the reliability of the intertied scenarios.**

Table of Contents

List of Figures

List of Tables

1 Introduction

Secure and reliable energy supply is essential to modern-day society. Power grids are responsible for the transmission and distribution of electric energy and traditionally, they are built in a centralized manner, where large-scale generation takes place in a central power plant and is then distributed to the customers around the power plant. The interconnection of individual power grids to a larger power grid can provide many advantages, such as more economic power plant operation, reduced peak loads, lower required plant reserve capacity, reduced capital and operation & maintenance (O&M) costs, as well as a more reliable power supply [2]. However, larger grids can also manifest challenges in voltage and frequency control as well single outages negatively affecting larger areas [2], [3].

For communities in remote locations it is infeasible to be connected to a regional or a national grid. Such communities are operated as islanded power systems, where the local generation must match the load at all times. These systems are often exposed to high power costs which result from high fuel costs, high installation costs, and a high degree of component redundancy, durability, and reliability to satisfy safety concerns. Those factors attributing to expensive power costs are directly influenced by the expensive costs to transport people and products to their remote destinations [4]. Consequently, an electrical intertie to centralize primary generation between nearby islanded microgrids will reduce the overall transportation costs for those villages.

Traditionally, transmission interties have operated with alternating current (AC) rather than direct current (DC) because the conversion devices necessary have not been readily available, proven, efficient and/or cost-effective. However, as the conversion technology improves, there can be advantages of using DC over AC [5]. DC interties only require two current carrying lines while AC lines need three current carrying lines, one for each phase. Furthermore, in AC the current tends to concentrate at the surface of the cable in what is called the skin effect, which increases the effective resistance for a given conductor size. This means DC transmission losses will be lower than AC losses for the same current and conductor size [6]. Finally, due to current required to charge the capacitance associated with cables, long distance AC transmission must be via overhead line. The DC line, however, can be buried underground between the two communities, reducing the required initial infrastructure costs, as well as future O&M costs. In addition to these economic advantages, DC interconnections more readily facilitate future integration of other DC technologies including battery energy storage systems.

MVDC transmission links have been considered for off-shore wind farms as an alternative to AC links [7]–[9]. These off-shore interties all assume a connection to a large on-shore grid but do not consider issues related to transmission between microgrids. A proposed MVDC connection between two islanded microgrids in Korea was examined using PSCAD/EMTDC and found that such an intertie, combined with energy storage, could improve stability and expand penetration of distributed generation sources compared to the independent systems [10]. The PSCAD/EMTDC software was used to simulate frequency and voltage transients in each microgrid caused by disruptions to the line, however long term economic considerations were not addressed over the lifetime of the project.

This study explores the feasibility and the potential cost benefit of a proposed electrical intertie between two islanded power systems located in northwest Alaska, Ambler and Shungnak. The configuration and background of the modeled intertie between the communities is very unique and is further described in the next section. Both medium voltage direct-current (MVDC) and medium-voltage alternating-current (MVAC) transmission lines are considered. The base case (or standalone case) is the current configuration of the communities, where each community generates its own power and no intertie exists. For the intertied scenarios, generation is centralized in Ambler, with only backup generation retained in Shungnak in case the intertie trips off line. To increase system reliability, the existing battery energy storage can be used in Shungnak to provide sufficient time to start a a diesel generator. In order to understand how the battery energy storage affects the value proposotion of the intertied scenarios, each scenario considers options both with and without battery energy storage.

A complete analysis for the intertie options must consider three aspects: economics, reliability, and power stability. The work presented in this paper focuses on the economics, with the addition of battery energy storage to address reliability concerns associated with the intertie. Stability of microgrids intertied with MVDC lines has been address previously [10]. Economic viability is demonstrated in this case study. It is shown that the installation cost of the intertie can be offset by the reduction in delivered fuel costs over the lifetime of the project, 30 years, with the MVDC intertie scenario achieving the lowest levelized cost of electricity (LCOE).

2 Case Study

Alaska has approximately 240 remote communities which are isolated from major roadways and power grids [11]. These islanded power systems are primarily powered by diesel generators and rely on long-distance fuel imports to the community. The costs associated with transportation and storage of diesel fuel results in high power generation costs.

The communities Ambler, Shungnak, and Kobuk in the Northwest Arctic Borough (NAB) in Alaska currently compose two islanded microgrids with some of the highest electricity costs in the state [12]. Currently, there is a 6 mile long medium-voltage alternating-current (MVAC) intertie between Shungnak and Kobuk. The entire load demand for the two communities is covered by generation in Shungnak. Henceforth, when Shungnak will be mentioned, Shungnak and Kobuk is intended. Shungnak is approximately 25 miles south-east from Ambler, and Kobuk is approximately 6 miles north-east from Shungnak. The population in Ambler is approximately 287 [13] while Shungnak's and Kobuk's approximate populations are 274 and 144, respectively [14], [15].

The meandering Kobuk river flows through Kobuk to Shungnak and to Ambler. For these communities seasonal river-transportation is the most cost-effective fuel delivery system [16]. However, upstream of Ambler, the Kobuk river is not always accessible for fuel barges due to shallow depth [16]. Additionally, the present diesel fuel storage (tank farms) in Ambler and Shungnak are not sufficient to store enough fuel to gap the longest duration between barge deliveries. Due to these complications in barge deliveries, both Ambler and Shungnak receive a substantial amount of fuel deliveries by plane, which increases the cost of fuel even further. On average, the reported cost of electricity for the past 10 years averaged 0.66 USD/kWh in Ambler and 0.73 USD/kWh in Shungnak and Kobuk. These costs are a factor 2.8 and 3.1 higher than the Alaska average, respectively, and a factor 4.7 and 5.2 higher than the national average, respectively [17]. An electrical intertie between Ambler and Shungnak could reduce the cost of power to the combined communities by centralizing power generation in Ambler and thus eliminating the need to fly in fuel to barge-inaccessible Shungnak. In addition, centralizing the generation in Ambler can help reduce operations and maintenance costs.

This case study evaluates three scenarios:

- continued stand-alone operation of the two communities;
- electrical interconnection via an overhead MVAC intertie (12.47 kV and 25 kV); and
- electrical interconnection via a buried MVDC intertie (15 kV and 25 kV).

For the base case, both Ambler and Shungnak will continue to self-generate their own power, thus both communities will receive tank farm upgrades. However, for the intertie scenarios, the entire generation for the two communities would be in Ambler, with the Shungnak power plant retained only for emergency operation. Thus, for the intertie scenarios, only Ambler will receive a tank farm upgrade.

The demand in these communities is primarily supplied by diesel generators. However, both communities have recently begun developing upon their diverse renewable energy resource potentials. In Ambler the majority of households have air-source heat pumps (ASHP) to complement the existing fuel-based heating system. The ASHP are combined with solar photovoltaic (PV) installations in the respective households [16]. In Shungnak, a 223kW bifacial solar PV array was recently installed [16] and is included in all three scenarios. In addition to the PV array, a 250kW/384kWh battery energy storage system (BESS) was also installed [16]. The impact of the BESS will be evaluated on how it contributes to system reliability and economics. Each scenario will consider and compare options with and without the BESS.

3 Methods

In this section the required data, the inputs for the models, as well as the employed methods for the power system and intertie modeling are presented.

3.1 HOMER

HOMER [18] is a popular tool for islanded power system energy balance and dispatch modeling [19]. HOMER allows a custom grid configuration, which requires the technical specifications of the different grid components, such as the generators (e.g. diesel generator, solar PV), any storage capacity and the load data.

For the modeling of the community grids, different data were required. Several parameters for diesel generators, the renewable energy installation, as well as the community load data in hourly resolution were provided by the electric utility in the communities, Alaska Village Electric Cooperative (AVEC) [1] and the NAB energy manager [16]. The used solar radiation and temperature timeseries are from the National Renewable Energy Laboratory (NREL) national solar radiation database [20] and available data from nearby meteorological stations [21], respectively. The particularity of the power system configuration required additional modeling to determine the electrical load resulting from the air-source heat-pumps (ASHP) in Ambler and the power generation from the bifacial solar PV installation in Shungnak.

The voltage drop across the intertie was determined for each scenario via a simplified Gauss-Seidel model [22]. With only two busses and a single line, the power flow systems of equations could be solved with a 1x1 matrix and relatively few iterations. Once the current through the lines is solved for, the line loss can be solved for as well. The voltage drop and line loss are considered in the energy balance modeling process.

Once the losses were calculated for the different transmission scenarios, an energy balance model was developed for each one using HOMER in order to simulate the microgrid system. The models examine both battery and no battery cases.

3.1.1 Controls

The microgrid dispatch controller is operated in Cycle Charging mode. In this mode the energy storage is charged and discharged to keep as many of the online generators operating at maximum rated capacity as possible, thereby maximizing fuel efficiency [23]. An alternative dispatch mode, Load Following, was not used in this model due to the relative sizing of the bifacial solar array. In Load Following mode the energy storage is only recharged in times of excess renewable energy [24]. In these scenarios, there are never occasions of excess renewable energy, therefore the BESS would go unused.

3.2 Electrical Load

The timeseries for the demand were provided by the local utility AVEC [1] for the year 2018 and are employed in an hourly resolution. The load in Ambler is 141 kW on average and reaches a peak load of 288 kW. In Shungnak the average load is 187 kW and the peak load is 336 kW. Both communities have a typical daily profile with increased usage during the day. The load also shows a clear seasonal profile, with decreased power usage during the summer and the highest demand during the winter months.

3.3 Diesel Generation

The diesel generator configuration for Ambler and Shungnak can be found in Tables 1 and 2, respectively. The installed generation capacity exceeds the load requirements because sufficient redundancy must be provided for the reliability of the grid.

The specific fuel consumption of the generators is determined by the generator efficiency, which in turn can vary depending on the operational loading of the generators (generators operating close to capacity are more efficient), as can be observed in figures A.1-A.3 in the appendix.

Generator	Capacity	O&M Costs
Cummins K19 G2	397 kW	2.60 US $/op. hour
Detroit Diesel S60	363 kW	2.28 US $/op. hour
Cummins K19 G2	271 kW	1.42 US $/op. hour

Table 1. Diesel generator configuration in Ambler, AK, including the diesel generator capacity and the modeled costs per operational hour

Generator	Capacity	O&M Costs
Cummins K19 G2	397 kW	2.60 US $/op. hour
Detroit Diesel S60	363 kW	2.28 US $/op. hour

Table 2. Diesel generator configuration in Shungnak, AK, including the diesel generator capacity and the modeled costs per operational hour

3.4 Bifacial Solar PV Generation

The 223 kW installed bifacial solar PV (Model 552 LG PV [16], [25]) in Shungnak is modeled as a power input profile, due to bifacial solar PV modeling not being implemented in HOMER. To model the power generation for the bifacial PV installation, two opposite-facing monofacial PV panels were modeled with local irradiance data from the Kobuk River Valley [20]. However, the resulting generation profile was then calibrated to more closely represent the installed bifacial PV by comparison to NREL's Solar Advisory Model (SAM) tool, which allows bifacial PV modeling for locations at lower latitudes, in the contiguous United States [26]. A direct comparison in SAM for a bifacial PV installation and that of two standard opposite-facing monofacial PV installations for the same location yielded a calibration factor. This factor was applied to the resulting generation from two opposite-facing monofacial PV installations modeled in Shungnak, resulting in an estimation for the yield of a bifacial PV installation in Shungnak.

3.5 Battery Energy Storage System

The 250kW/384kWh Blue Ion LX battery system from Blue Planet Energy was also installed along side the bifacial PV array in Shungnak. The system uses a lithium iron phosphate chemistry and is also capable of operating the grid while the diesel generators are off. The BESS was modeled as 36 strings of the Sonnen Batterie eco 10 from the HOMER Pro energy storage catalog. The eco 10 was selected in order to match the battery chemistry and rated duration of the actual system. Each string has nominal ratings of 240 V, 7 kW, and 10 kWh, therefore 36 strings will approximate the power and energy ratings of the installed BESS.

3.6 Air-Source Heat Pump Electrical Usage Modeling

The community of Ambler recently installed air-source heat pumps (ASHP) to complement the fuel-based burner stoves [27] for the heating demand. The ASHP electrical usage is a function of the heating demand and the temperature-dependent coefficient of performance. According to communications with the NAB [16], the ASHP can be operated for outside temperatures down to 0°F, below which the regular fuel burners would cover the entire heating demand. The total annual residential heating demand was determined from annual residential heating fuel consumption [16] and then distributed according to heating degree hours, assuming a residential heating threshold at 65°F (18°C). The modeled ASHP were fully allocated to serve the heating demand during periods with temperatures above 0°F, in consideration of general temperature-based coefficient of performance (COP) values [28] for ASHP. Thus, the resulting synthetic electrical usage specific to the modeled ASHP shows an hourly profile that considers the operational limits of the ASHP.

3.7 Transmission Line Modeling

For each of the two intertie scenarios, two voltage levels are considered: 15 kV, 25 kV, 12.47 kV, and 25 kV. The AC voltages are commonly used for lines operated by AVEC carrying similar loads [1] and comparable values were selected for the DC lines. Table 3 shows properties of the transmission lines used in these four intertie scenarios. Included are the resistance[1] per unit length at 25 °C, R, and the geometric mean radius, GMR, of the AC lines.

Scenario	Line Type	$R(\Omega/\text{kft})$	$GMR(\text{ft})$
12.47 kV	1/0 ACSR [29]	0.163	0.0059
25 kV	1/0 ACSR [29]	0.163	0.0059
15 kV	#2 AWG Al Cable [30]	0.267	-
25 kV	1/0 Al Cable [30]	0.168	-

Table 3. Transmission line parameters used to calculate voltage drop and power losses.

3.7.1 Transmission Line Power Losses and Voltage Drops

The power losses and voltage drop across the DC transmission line were modeled assuming each segment was composed of resistive, R, components. The AC lines were assumed to have resistive, R, and inductive, X, components. The values of R and X depend on the type, configuration, and length of the lines. For the AC calculations, it is assumed there are three balanced phases operating at 60 Hz. Since they are balanced there is no voltage drop or power loss along the neutral phase. The value of X is calculated as $X = 2\pi f L$, where f is the AC frequency and L is the per-phase inductance. L is calculated as

$$L = 2 \times 10^{-7} \ln \frac{GMD}{GMR} (\text{H/m}) \tag{3.1}$$

where GMD is the geometric mean distance between the phases and GMR is the geometric mean radius of the lines [22]. GMD is assumed to be 4.41 ft for 12.47 kV lines and 5.64 ft for the 25 kV lines. GMR is determined by the size and stranding of the lines and the values used are specified in Table 3.

In each scenario, voltage drops at max load are calculated and the power loss is calculated for each 1 hour time step over the course of one year and summed. The voltage drops were computed to ensure practical system design. The hourly power losses were computed and added to the underlying load profiles as entered into HOMER in order to properly account for increased fuel consumption due to intertie losses. For the calculations, first the DC and AC currents are calculated as

$$I_{DC} = \frac{P}{V_{DC}} \text{ and} \tag{3.2}$$

$$I_{AC} = \frac{P}{\sqrt{3} V_{AC} \cos\phi}. \tag{3.3}$$

The voltage drops are calculated as

$$\Delta V_{DC} = 2 R I_{DC} \text{ and} \tag{3.4}$$

$$\Delta V_{AC} = \sqrt{3} I_{AC} (R\cos\phi + X\sin\phi). \tag{3.5}$$

The power losses are calculated as

$$P_{loss,DC} = 2 R I_{DC}^2 \text{ and} \tag{3.6}$$

$$P_{loss,AC} = 3 R I_{AC}^2. \tag{3.7}$$

[1] AC resistances used for AC lines and DC resistance for DC lines which may differ due to skin effect.

To calculate the AC voltage drop at maximum load the power factor was assumed to be 0.8, which corresponds to a phase angle, $\phi = 0.64$ rad. The power factor when calculating the average AC line losses was assumed to be 0.9, which corresponds to a phase angle, $\phi = 0.45$ rad.

However, the initial current calculation does not take the voltage drop across the lines into account. These loads draw the same amount of power regardless of the voltage level, therefore the current drawn by the load would actually be greater than the initial calculation. To account for this, the voltage drop equations were iterated until the progressively higher current estimates converged.

Table 4 shows the percent voltage drop at maximum load relative to the rated voltage and percent line losses relative to the annual load. It is important to note conductor size when interpreting the results. Although #2 conductor would have sufficient ampacity, 1/0 is used for both the AC cases according to standard design and was also the smallest conductor size available for the 25 kV cable. Thus the 15 kV DC scenario has the largest voltage drop and highest losses. The voltage drop and losses for the 25 kV DC case are also slightly greater than for the 25 kV AC case due to the higher current required to carry same amount of power across two vs. three lines.

Type	Operating voltage	Conductor size	Voltage drop at max load	Average line losses
DC AL Underground	15 kV	#2 AWG	12.0%	6.2%
	25 kV	1/0	2.5%	1.4%
AC ACSR Overhead	12.47 kV	1/0	8.7%	3.4%
	25 kV	1/0	2.0%	0.8%

Table 4. Percent voltage drop at maximum load and percent annual power loss across different transmission line scenarios from Ambler, AK to Shungnak, AK.

3.8 Power System Costs

The intent of this study was to evaluate the relative economics of the stand-alone vs. intertied scenarios. Considered costs included installed cost of the interties and bulk fuel tanks, operation and maintenance (O&M) costs, and fuel costs. In the following sections, some of the costs are presented in more detail. The renewable energy generation and energy storage components are equal in all scenarios, as the focus lies in the comparison of the standalone case with the different intertie scenarios. Hence, the installation costs for renewable energy and energy storage components were not considered in the modeling process, as these components are already part of the existing power system configuration. However, relevant operation, maintenance, and/or replacement costs are included.

3.8.1 Diesel Generators

The diesel generators have an essential role in the islanded power systems, as they cover the largest part of the load and, together with diesel fuel, represent a substantial amount of the final cost of energy. The total O&M cost estimate for the diesel generators is obtained from the local utility, AVEC [1] and includes the hourly operational costs (e.g. lube) and the overhaul costs, which are distributed over the total generated energy over the estimated lifetime of the generator.

The non-fuel operating costs of the diesel generators in Ambler and Shungnak are shown in Tables 1 and 2, respectively. The modeled diesel fuel costs highly depend on the delivery location, and are also exposed to yearly price fluctuations. The fuel costs used for the different scenarios can be observed in Table 5 [16].

Scenario	Fuel Cost (US $/gal)	
	Ambler	Shungnak
Base Case	3.71	6.15
Intertie	3.71	-

Table 5. Modeled fuel cost for the different scenarios and the delivery locations of Ambler and Shungnak [16].

The fuel cost in Ambler is the same for both the base case and intertie scenarios because a tank farm upgrade, considered as a necessity in both the base case and the intertie scenarios, would allow barged fuel delivery to Ambler. Although a tank farm upgrade is also considered for Shungnak in the base case, a large amount of deliveries would still be required by plane, due to the water level of the Kobuk river. The tank farm upgrades costs are estimated to be 10 million USD in Ambler and 2.7 million USD in Shungnak [16]. Consequently, the total tank farm upgrade for the base case scenario is 12.7 million USD in total, as both tank farms require an upgrade in this scenario alone.

3.8.2 Energy Storage Costs

As previously indicated, the initial capital costs of the BESS are assumed to be zero. The base replacement costs at years 10 and 20 of the project lifetime were assumed to be $16,000 per string or $576,000 for the whole system.

3.8.3 Intertie Installation Costs

The installed costs of the MVAC and the MVDC intertie are shown in Table 6. For the overhead MVAC intertie, the cost is based on experience values and estimation from AVEC [1] and from NAB [16]. Actual overhead installation costs will depend on topography, climate, vegetation, and soil, with the highest costs occurring for installation over boggy areas. In these areas, equipment including utility poles and conductors, must be delivered and installed during the winter months when the ground is frozen to prevent damage to the tundra. For this case study, it is expected the overhead MVAC installation costs will be near the high end of the listed range due to the wide distribution of muskeg and permafrost. These installations will also incur higher O&M costs as poles become loose.

In the case of the buried MVDC intertie, there is no regional experience to provide an estimated range of costs. Thus, the installed cost for the buried MVDC intertie is based on a detailed project budget developed by personnel with decades of experience with construction projects in remote Alaska with the cooperation of key manufacturers. Key aspects of the installation include identification of a proven commercially available 500 kW medium voltage converter, equipment typically only available down to the tens of MW; the use of amphibious equipment to allow favorable summer deployment and burial of the cable without damaging the muskeg; and the use of armored 25 kV cable heavy enough to remain buried during the summer thaw and protected against freeze/thaw events and animals. Table A.4, located in appendix A.0.2, shows the detailed breakdown of installation costs for the MVDC intertie based on manufacturer quotes and experiences gathered in coordination with the Alaska Center for Energy and Power (ACEP), and AVEC [1].

Cost Breakdown	Overhead MVAC	Buried MVDC
Intertie installed cost per mile	$ 350k - 750k	$ 232k
Substations installed cost	$ 200k	-
Converters installed cost	-	$ 1,100k
Total cost for 25 mile intertie	$ 8,950k -18,950k	$ 6,892k

Table 6. Breakdown of intertie installation costs

4 Results

The modeling tool HOMER provides several output metrics that allow to compare the different scenarios and different sensitivities. In this section the most important metrics are presented and discussed.

4.1 Cost of Electricity

The levelized cost of electricity (LCOE) distributes all incurred (installation, O&M, and other costs) during the modeling lifetime (30 years in this case study) among the total delivered energy, thus, providing an intuitive and important metric to compare different scenarios with. Figure 1 shows the modeling results for the different scenarios with and without the BESS. The results for the Base Case (average of Ambler and Shungnak, weighted by total yearly energy use) represent the current actual configuration of the communities [12], [31], [32] in addition to the tank farm upgrades necessary in both communities. The intertie scenarios include the installed costs of the interties. The range presented for the MVAC LCOE is due to uncertainty of installation costs, as discussed in section 3.

	Scenario	LCOE without BESS (US $/kWh)	LCOE with BESS (US $/kWh)
Base Case	-	0.697	0.706
MVAC Intertie	12.47 kV	0.719 - 0.850	0.726 - 0.857
MVAC Intertie	25 kV	0.715 - 0.846	0.723 - 0.854
MVDC Intertie	15 kV	0.678	0.685
MVDC Intertie	25 kV	0.672	0.680

Table 7. Levelized cost of electricity, without and with a BESS, for different scenarios, considering the base case, the projected MVAC interties, and the projected MVDC interties.

The bar chart in Figure 1 graphically represents the results shown in table 7. The modeled LCOE for both MVDC scenarios is substantially lower than the LCOE for MVAC scenarios, even at the low end of the cost range. The 25 kV DC case is lower cost than both the 15 kV DC case the standalone reference case.

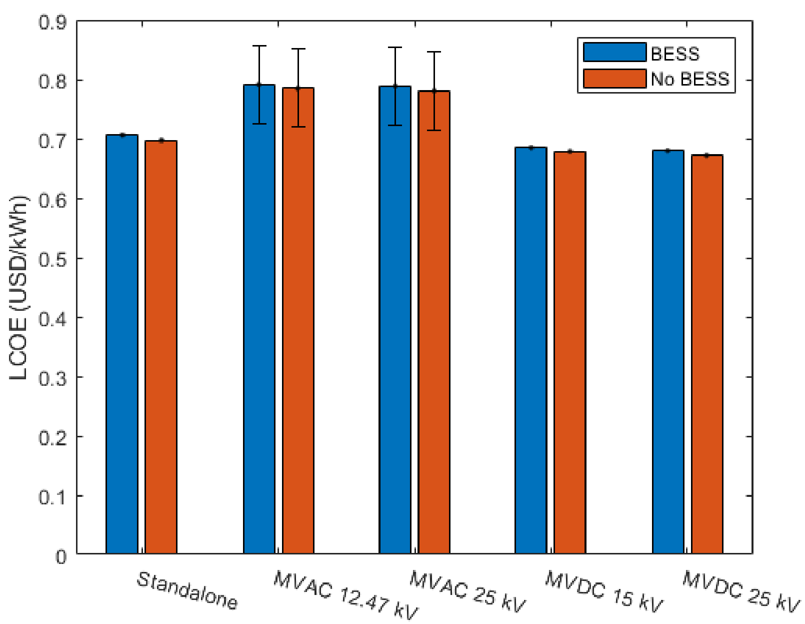

Figure 1. Modeled Levelized Cost of Electricity of the communities Ambler and Shungnak for the standalone (base case) scenario and the intertie scenarios (MVAC and MVDC) with different line voltages. The MVAC range results from uncertainty of installation costs.

The advantage of the both MVAC and MVDC scenarios is mainly provided by the avoidance of expensive fuel deliveries to Shungnak. The high installation costs for both intertie scenarios are balanced by the lower operational (fuel costs) costs, as fuel is only delivered to Ambler. Assuming the lifetime of the intertie to exceed the modeling lifetime of 30 years, the value provided by the intertie would further decrease the LCOE, compared to the standalone case.

The BESS contributes to system reliability in all scenarios. For the base case scenario, the BESS contributes to reliability in Shungnak by providing spinning reserve if a generator fails; for both the intertied scenarios, the BESS contributes to reliability by providing spinning reserve should the intertie fail, giving time to start a backup generator in Shungnak. Although the inclusion of the BESS adds to the levelized cost in all scenarios (due to the additional cost to replace the storage at ten year intervals outweighing the economic benefits of operating the diesel generators at more efficient loading levels), the most important thing to note is that the MVDC scenario with BESS is still cheaper than the stand-alone scenario without BESS. Finally, a BESS could also provide stability in response to fluctuations in renewable power generation. However the one hour timescale used in these simulations is too large to capture the fluctuations.

4.2 Fuel use

Fuel costs represent a large part of the final expenses incurred during generation, thus, it is interesting to compare fuel usage among the different scenarios. In the base case, the HOMER results show a yearly diesel fuel consumption of approximately 720k liters.

The average losses from the different intertie scenarios range between 0.8% and 6.2% (as seen in Table 4), while the baseline scenario has no transmission losses. However, the fuel use in all intertie cases is less than that of the base case. In the case of the intertie with the least transmission losses (MVAC 25 kV), fuel usage is reduced by approximately 6.4%, whereas the MVDC 15 kV intertie with the highest losses sees a fuel use reduction by 3.5%, compared to the base case. The fuel use reduction despite the transmission losses is due to the generator operational loading. In the base case the diesel generators must sometimes operate at a lower loading which achieves a lower fuel efficiency than if the generators were ran at their rated optimal loading (fuel efficiency values for generators are shown in figures A.1-A.3 in appendix A.0.1). In the intertie cases fewer generators cover the entire demand, which allows the generators to run at more optimal operational loading. Consequently, according to the model outputs, the increase in fuel efficiency slightly outweighs the transmission line losses.

5 Conclusions

This work analyses the effects of the potential interconnection of islanded power systems in the case study of an electrical intertie between the remote communities of Ambler and Shungnak in Alaska's Northwest Arctic Borough. The study compares the current standalone case of the communities with an MVDC and an MVAC intertie using HOMER Pro software to simulate each scenario. The case study shows that the high installation costs for the interties are mostly counterbalanced by the reduction in fuel costs, due to fuel delivery cost reductions, with the 25 kV MVDC intertie scenario yielding the lowest levelized cost per kilowatt-hour.

The interties allow the diesel generators in the community of Ambler to run more efficiently, due to sharing of the load for the communities. The increase in efficiency due to more optimal loading of the generators in the intertie cases outweighs the line losses of the intertie. Considering the two intertie scenarios, the modeled MVDC buried intertie installation and O&M costs are lower than the modeled costs for the MVAC overhead intertie, resulting in lower costs of electricity. Although the MVDC scenarios required the additional power conversion equipment, this was outweighed by the significantly higher installation costs of the overhead AC lines. Consequently, for this case study, the MVDC lines result in the lowest cost of energy of all scenarios for the modeling lifetime.

The addition of a BESS to each of these scenarios consistently increased the levelized cost of electricity. While the increased efficiency of the generators was able to outweigh the transmission losses and added cost of the 25 kV MVDC intertie, the marginal benefit of the BESS was less than its cost of replacement. However, the levelized cost of 25 kV MVDC intertie scenario with a BESS is still less than that of the stand alone baseline and MVAC scenarios, with or without a BESS. Furthermore, additional renewable energy resources could increase the value of the BESS by being able to store excess energy which would otherwise be lost. Additionally, the location of the energy storage in Shungnak can provide reliability to the community in the event of an intertie failure. Lastly, the BESS could be used to mitigate the fluctuations caused by solar generation at shorter time scales, as shown in [10].

This work has provided additional motivation for local stakeholders to consider installation of an MVDC intertie between Shungnak and Ambler. Future work will examine the effects of incorporating run of the river hydro resource from the nearby Kogoluktuk River. This will require additional intertie infrastructure, but also provide opportunity for subtantially greater fuel savings and consideration of seasonal energy storage. Additionally, further examination of reliability is warrented. Considering statistically occurring contingent operations involving the Shungnak BESS and diesel generators can inform how system reliability impacts lifetime economics.

Finally, it is important to note that the economics of an electrical interconnection between two or more remote communities will be significantly affected by location, notably accessibility and terrain, distances between communities, and specifics of the individual power systems. This case study has provided a valuable data point exposing the possibilities. However, as with renewable integration studies, site-specific modeling would be required to evaluate intertie options in other remote regions.

References

[1] W. Thomson, *Personal conversation and email exchange*, 2021.
[2] Electrical Article, RAVI, *Interconnected Power System: Advantages, Disadvantages, and Problems*, http://electricalarticle.com/interconnected-power-system-advantages-disadvantages-and-problems/, accessed on 22-10-2021.
[3] J. Hostetter, "What trends are driving growth for the microgrid market?" *Microgrid Knowledge*, 2020. DOI: https://microgridknowledge.com/microgrid-market-growth-ameresco/.
[4] G. Holdmann, R. Wies, and J. Vandermeer, "Renewable energy integration in alaska's remote islanded microgrids: Economic drivers, technical strategies, technological niche development, and policy implications," *IEEE*, vol. Vol. 107, No. 9, 2019. DOI: 10.1109/JPROC.2019.2932755.
[5] The Alaska Center for Energy and Power, *Small-Scale High Voltage Direct Current*, https://acep.uaf.edu/media/62339/ACEP-HVDC-Phase-2-Final-Report.pdf, 2013.
[6] M. Starke, L. M. Tolbert, and B. Ozpineci, "AC vs. DC Distribution: A Loss Comparison," in *2008 IEEE/PES Transmission and Distribution Conference and Exposition*, IEEE, 2008, pp. 1–7, ISBN: 978-1-4244-1903-6. DOI: 10.1109/TDC.2008.4517256. [Online]. Available: http://ieeexplore.ieee.org/lpdocs/epic03/wrapper.htm?arnumber=4517256.
[7] M. S. Carmeli, F. Castelli-Dezza, D. Rosati, G Marchegiani, and M. Mauri, "Mvdc connection of offshore wind farms to the transmission system," in *SPEEDAM 2010*, IEEE, 2010, pp. 1201–1206.
[8] G. Abeynayake, G. Li, J. Liang, and N. A. Cutululis, "A review on mvdc collection systems for high-power offshore wind farms," in *2019 14th Conference on Industrial and Information Systems (ICIIS)*, IEEE, 2019, pp. 407–412.
[9] M. R. Islam, M. A. Rahman, K. M. Muttaqi, and D. Sutanto, "A new magnetic-linked converter for grid integration of offshore wind turbines through mvdc transmission," *IEEE Transactions on Applied Superconductivity*, vol. 29, no. 2, pp. 1–5, 2019.
[10] J. Ahn and E. H. Kim, "Implementation of a Microgrid Scheme Using a MVDC Connection Between Gapado Island and Marado Island in South Korea," *Energies*, vol. 12, no. 1, 2019, ISSN: 19961073. DOI: 10.3390/en12010187.
[11] S. T. Lacey, *Census Bureau*, https://www.census.gov/library/stories/2019/07/alaska-remote-areas-always-first-counted-decennial-census.html, accessed on 03-11-2021.
[12] Alaska Energy Authority, *Power cost equalization (pce), 2019*, http://www.akenergyauthority.org/LinkClick.aspx?fileticket=qgKDRJywe2M%3d&portalid=0, accessed on 03-11-2021.
[13] Northwest Arctic Borough, Ambler, *NWAB*, https://www.nwabor.org/village/Ambler/, accessed on 22-12-2021.
[14] Northwest Arctic Borough, Shungnak, *NWAB*, https://www.nwabor.org/village/Shungnak/, accessed on 22-12-2021.
[15] Northwest Arctic Borough, Kobuk, *NWAB*, https://www.nwabor.org/village/Kobuk/, accessed on 22-12-2021.
[16] N. A. B. E. M. Ingemar Mathiasson, *Personal conversations and interactions during case study duration*, 4-10-2021.
[17] EIA, *Alaska State Energy Profile.* https://www.eia.gov/state/print.php?sid=AK, accessed on 03-12-2021.
[18] HOMER, *Homer software*, https://www.homerenergy.com/, accessed on 06-12-2021.
[19] VECKTA, *5 microgrid / des hurdles and how to overcome them*, https://www.veckta.com/2020/08/06/5-microgrid-hurdles-and-how-to-overcome-58them/, accessed on 06-12-2021.
[20] NREL, *Nrel pv watts*, https://pvwatts.nrel.gov/, accessed on 12-22-2021.
[21] Iowa State University, *Iowa Environmental Mesonet*, https://mesonet.agron.iastate.edu/request/download.phtml?network=AK_ASOS, accessed on 22-10-2021.
[22] J. D. Glover, T. J. Overbye, and M. S. Sarma, *Power system analysis & design*. Cengage Learning, 2017.
[23] HOMER, *Homer pro cycle charging strategy*, https://www.homerenergy.com/products/pro/docs/latest/cycle_charging_strategy.html, accessed on 06-10-2022.
[24] HOMER, *Homer pro load following strategy*, https://www.homerenergy.com/products/pro/docs/latest/load_following_strategy.html, accessed on 06-10-2022.
[25] LG Electronics, *NeON2 Bifacial*, https://www.lg.com/jp/images/solar/download/DS_NeON2-BiFacial_60cells.pdf, accessed on 12-22-2021.

[26] National Renewable Energy Laboratory, *Nrel system advisory model*, https://sam.nrel.gov/, accessed on 12-27-2021.
[27] Toyotomi, *Heating Products Catalog*, https://toyoheat.com/products/, accessed on 23-10-2021.
[28] CCHRC, *Airsource Heat Pump Homeowner Education Class*, 2021.
[29] Prysmian Group, *Transpowr acsr bare overhead conductor*, https://na.prysmiangroup.com/node/21463, accessed on 12-08-2021.
[30] The Okonite Company, *"engineering handbook"*, http://www.okonite.com/media/catalog/product/files/EHB_2018.pdf#page=8, accessed on 12-08-2021, 2018.
[31] Alaska Energy Authority, *Power cost equalization (pce), 2018*, http://www.akenergyauthority.org/LinkClick.aspx?fileticket=qgKDRJywe2M%3d&portalid=0, accessed on 03-11-2021.
[32] Alaska Energy Authority, *Power cost equalization (pce), 2020*, http://www.akenergyauthority.org/LinkClick.aspx?fileticket=qgKDRJywe2M%3d&portalid=0, accessed on 03-11-2021.
[33] XENDEE, *Microgrid design support platform*, https://xendee.com/, accessed on 06-12-2021.
[34] Wetland Equipment Company, *Quote from vendor*, 2021.
[35] The Okonite Company, *Quote from vendor*, 2021.
[36] Resilient Power, *Quote from vendor*, 2021.
[37] R. Arisyadi, "A Progressive Alternative of Energy Planning for West Sumatera Province," *IOP Conference Series: Earth and Environmental Science*, vol. 753, no. 1, p. 012 032, 2021, ISSN: 1755-1307. DOI: 10.1088/1755-1315/753/1/012032. [Online]. Available: https://iopscience.iop.org/article/10.1088/1755-1315/753/1/012032.
[38] S. Ashfaq, D. Zhang, C. Zhang, and Z. Y. Dong, "Regionalisation of Islanded Microgrid Considering Planning and Operation Stages," *IET Renewable Power Generation*, vol. 14, no. 1, pp. 145–153, 2020, ISSN: 1752-1416. DOI: 10.1049/iet-rpg.2019.0894. [Online]. Available: https://onlinelibrary.wiley.com/doi/10.1049/iet-rpg.2019.0894.

Appendix A Model Parameters

A.0.1 Diesel Generator Fuel Efficiency

Nominal Generator Capacity (%)	Fuel Efficiency (%)
10	18.0
20	26.0
30	30.5
40	33.2
50	35.3
60	36.4
70	37.2
80	37.9
90	38.4
100	38.9

Table A.1. Electric fuel efficiency employed for diesel generator 397 kW [1]

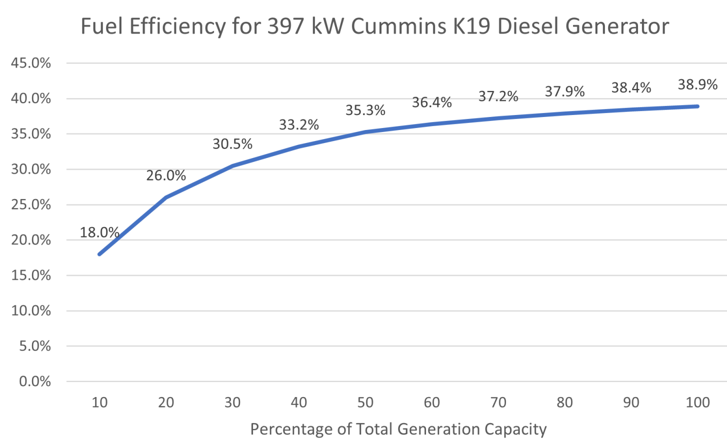

Figure A.1. Fuel efficiency for 397 kW Diesel Generator model.

Nominal Generator Capacity (%)	Fuel Efficiency (%)
10	23.5
20	33.2
30	37.1
40	39.9
50	41.1
60	42.9
70	42.6
80	42.6
90	42.4
100	42.4

Table A.2. Electric fuel efficiency employed for diesel generator 363 kW [1]

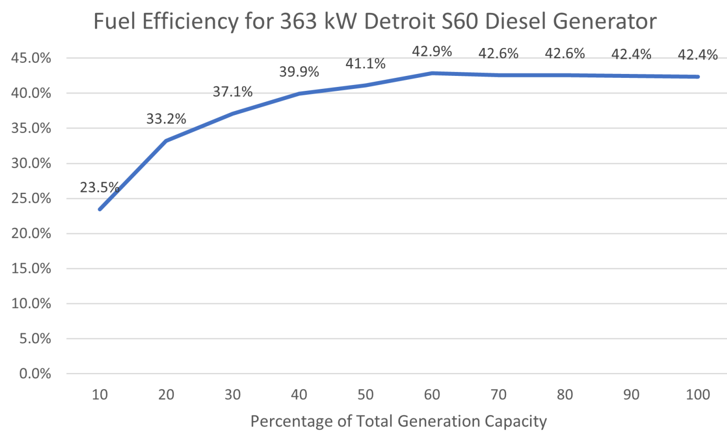

Figure A.2. Fuel efficiency for 363 kW Diesel Generator model.

Nominal Generator Capacity (%)	Fuel Efficiency (%)
10	19.9
20	28.5
30	33.3
40	36.2
50	38.2
60	39.5
70	40.3
80	41.2
90	41.5
100	42.1

Table A.3. Electric fuel efficiency employed for diesel generator 271 kW [1]

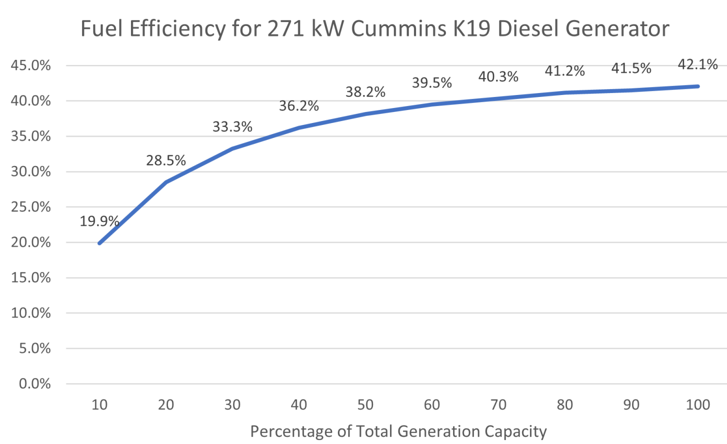

Figure A.3. Fuel efficiency for 271 kW Diesel Generator model.

A.0.2 MVDC Cost Breakdown

Category / Item	Itemized Cost	Category Cost
Two 500 kW 480 Vac / 25 kVdc converters (Resilient Power Systems [36])	$ 1,100k	-
1/0 25 kV armored cable on steel reels (The Okonite Company [35])	$ 1,128k	-
Misc (concrete, splicing materials, field work enclosures)	$ 99k	-
Materials Total	-	$ 2,327k
Amphibious trencher platform (Wetland Equipment Company [34])	$ 715k	-
Amphibious excavator (Wetland Equipment Company [34])	$ 550k	-
Bulldozer (rental) and Side by Side	$ 31k	-
Equipment Total	-	$ 1,296k
Labor Total (Preconstruction, mobilization, field work, and demob)	-	$ 543k
Mobilization and Demobilization Total	-	$ 110k
Services Total (Freight, travel, commissioning support)	-	$ 562k
Overhead, General and Administrative, Fee, Contingency, and Tax	-	$ 2,055k
Total		**$ 6,892k**

Table A.4. Detailed breakdown of installation costs for buried MVDC intertie